

# Effective Connectivity Reveals Right-Hemisphere Dominance in Audiospatial Perception: Implications for Models of Spatial Neglect

Martin J. Dietz,<sup>1</sup> Karl J. Friston,<sup>2</sup> Jason B. Mattingley,<sup>3,4</sup> Andreas Roepstorff,<sup>1</sup> and Marta I. Garrido<sup>2,3</sup>

<sup>1</sup>Centre for Functionally Integrative Neuroscience, Institute of Clinical Medicine, Aarhus University, 8000 Aarhus C, Denmark, <sup>2</sup>Wellcome Trust Centre for Neuroimaging, University College London, London WC1N 3BG, United Kingdom, <sup>3</sup>Queensland Brain Institute and Australian Research Council Centre of Excellence for Integrative Brain Function and <sup>4</sup>School of Psychology, The University of Queensland, St Lucia 4072, Brisbane, Australia

Detecting the location of salient sounds in the environment rests on the brain's ability to use differences in sounds arriving at both ears. Functional neuroimaging studies in humans indicate that the left and right auditory hemispheres are coded asymmetrically, with a rightward attentional bias that reflects spatial attention in vision. Neuropsychological observations in patients with spatial neglect have led to the formulation of two competing models: the orientation bias and right-hemisphere dominance models. The orientation bias model posits a symmetrical mapping between one side of the sensorium and the contralateral hemisphere, with mutual inhibition of the ipsilateral hemisphere. The right-hemisphere dominance model introduces a functional asymmetry in the brain's coding of space: the left hemisphere represents the right side, whereas the right hemisphere represents both sides of the sensorium. We used Dynamic Causal Modeling of effective connectivity and Bayesian model comparison to adjudicate between these alternative network architectures, based on human electroencephalographic data acquired during an auditory location oddball paradigm. Our results support a hemispheric asymmetry in a frontoparietal network that conforms to the right-hemisphere dominance model. We show that, within this frontoparietal network, forward connectivity increases selectively in the hemisphere contralateral to the side of sensory stimulation. We interpret this finding in light of hierarchical predictive coding as a selective increase in attentional gain, which is mediated by feedforward connections that carry precision-weighted prediction errors during perceptual inference. This finding supports the disconnection hypothesis of unilateral neglect and has implications for theories of its etiology.

**Key words:** audiospatial; Bayesian; connectivity; DCM; EEG; neglect

## Introduction

The brain's ability to use spectral, phase, and energy differences between sounds arriving at the left and right ears is crucial for locating sounds in the environment. The main cue, for inferring the source of a sound in the horizontal plane, is the interaural time delay (ITD) between the two ears (Thompson et al., 2006). Left and right auditory afferents are known to converge early in

the auditory hierarchy, at the level of the superior olivary complex in the brainstem, and then project to the medial geniculate nucleus of the thalamus via the inferior colliculus in the midbrain (Irvine, 1986; Heffner and Masterton, 1990). Functional neuroimaging studies in humans have shown that the inferior colliculus (Thompson et al., 2006) and the primary auditory cortex (von Kriegstein et al., 2008) elicit stronger responses in the hemisphere contralateral to the side of space where the stimulus is perceived. This is consistent with the anatomical crossing of fiber pathways up to the level of the cerebral cortex where interhemispheric integration becomes transcallosal. Several neuroimaging studies indicate that the cortical systems that mediate audiospatial perception are organized asymmetrically beyond primary auditory cortex, with a right-hemispheric specialization. Specifically, the right inferior parietal cortex has consistently been shown to respond to both contralateral and ipsilateral stimuli with fMRI (Griffiths et al., 1998; Bushara et al., 1999; Maeder et al., 2001; Krumbholz, 2005; Brunetti et al., 2008), positron emission tomography (Zatorre et al., 2002), and magnetoencephalography (MEG; Kaiser et al., 2000). This functional asymmetry parallels spatial attention in vision (Corbetta and Shulman, 2002). Converging evidence thus points to the hemispheric specialization of spatial attention as a multimodal property of the brain (Fritz et

Received Sept. 3, 2013; revised Feb. 13, 2014; accepted Feb. 21, 2014.

Author contributions: M.J.D. designed research; M.J.D. performed research; M.J.D., K.J.F., J.B.M., A.R., and M.I.G. contributed unpublished reagents/analytic tools; M.J.D. analyzed data; M.J.D., K.J.F., and M.I.G. wrote the paper.

M.J.D. is supported by the Danish Agency for Science, Technology, and Innovation. K.J.F. is supported by the Wellcome Trust. J.B.M. is supported by an Australian Research Council Laureate Fellowship (FL110100103) and a Project Grant from the National Health and Medical Research Council (APP1034110). A.R. is funded by the Danish Agency for Science, Technology, and Innovation's University Investment Grant to MINDlab and M.I.G. is supported by an Australian Research Council Discovery Early Career Researcher Award (DE130101393). We thank Chris Frith and two anonymous reviewers for their valuable comments.

The authors declare no competing interests.

This article is freely available online through the *J. Neurosci.* Author Open Choice option.

Correspondence should be addressed to Martin J. Dietz, Centre for Functionally Integrative Neuroscience, Institute of Clinical Medicine, Aarhus University, 8000 Aarhus C, Denmark. E-mail: martin@cfi.au.dk.

DOI:10.1523/JNEUROSCI.3765-13.2014

Copyright © 2014 Dietz et al.

This is an Open Access article distributed under the terms of the Creative Commons Attribution License (<http://creativecommons.org/licenses/by/3.0>), which permits unrestricted use, distribution and reproduction in any medium provided that the original work is properly attributed.

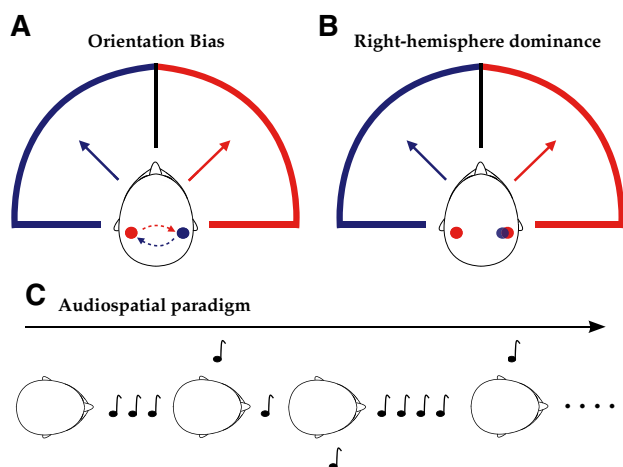


**Figure 1.** *A*, Orientation bias model. *B*, Right-hemisphere dominance model. *C*, Auditory location oddball paradigm.

al., 2007), which dominates current theories of unilateral neglect (Mesulam, 1999). Neglect of the left side of the sensorium after a right-hemisphere lesion is more frequent and severe than vice versa (Driver and Mattingley, 1998). While the etiology of this phenomenal asymmetry remains unresolved, two alternative accounts have been proposed (Fig. 1): the orientation bias model hypothesizes that attention is shifted toward the contralateral side of space via inhibition of the ipsilateral hemisphere (Kinsbourne, 1970, 1977) and the right-hemisphere dominance model states that the left hemisphere represents the right side of space, whereas the right hemisphere represents both sides of the sensorium (Mesulam, 1999).

To disambiguate between these two hypotheses, we used an oddball paradigm, where the location of a sound changed sporadically and unpredictably from the midline to the left or to the right side of space. We formulated a set of dynamic causal models (DCMs) that map onto the orientation bias model or the right-hemisphere dominance model, respectively. These models represent alternative hypotheses about the cortical networks that mediate audiospatial perception and make different assumptions about the type neuronal connections that embody hemispheric asymmetries in a frontoparietal network. We used Bayesian model selection to compare the evidence for the orientation bias and the right-hemisphere dominance models with varying levels of complexity in terms of their forward and backward connections.

## Materials and Methods

**Experimental design and data acquisition.** We recorded 64-channel electroencephalography (EEG) from 12 healthy volunteers (seven females, mean age 25 years, range 20–35) using active Ag/AgCl electrodes placed according to the extended 10–20% system (Brain Products). Subjects were presented with an auditory oddball paradigm in which the location of a sound changed unpredictably from midline to the left and right side of egocentric space (Fig. 1C). Stimuli perceived as originating from the midline were repeated between four and seven times and had 80% probability of occurrence. An ITD of 800  $\mu$ s between left and right ears was used to induce a change in the location of the stimulus to subjective left and right space at  $\sim 90^\circ$  angle in the horizontal plane. Stimuli at left and right locations each had 10% probability of occurrence. All other spectral, amplitude, and duration parameters were kept constant. Stimuli consisted of sinusoidal pure tones with 75 ms duration, including 5 ms fade-in and 5 ms fade-out. We used Presentation software (Neurobehavioural Systems) to deliver stereo stimuli through in-ear headphones

(Sennheiser) at a stimulus-onset asynchrony of 500 ms. Each subject was presented with  $\sim 1400$  midline trials, 200 left and 200 right hemispace trials. Participants were instructed to maintain fixation on a central cross (on a black screen) during the experiment. Ethical approval was obtained from the local ethics committee of the Central Denmark Region and subjects gave their informed consent before the experiment.

**EEG data preprocessing.** Data analysis was performed using Statistical Parametric Mapping (SPM8) academic software (Wellcome Trust Centre for Neuroimaging, UCL; <http://www.fil.ion.ucl.ac.uk/spm/>) implemented in MATLAB (MathWorks.). EEG data were re-referenced to the average over sensors, high-pass filtered at 0.5 Hz, and low-pass filtered at 30 Hz using a two-pass Butterworth filter and downsampled from 1 kHz to 250 Hz. Experimental trials were epoched from  $-100$  to  $400$  ms in peristimulus time and baseline corrected using the average over the pre-stimulus time window. Artifacts were rejected by thresholding the signal at  $80 \mu$ V, leaving a total of 80% trials on average. Trials were averaged using robust averaging (Wager et al., 2005) to form evoked responses (ERPs). To facilitate analysis in sensor space, the ERPs were converted into 3D spatiotemporal images (2D scalp plus the time dimension) and smoothed with a Gaussian kernel of 20 mm FWHM in the spatial and 20 ms in the temporal dimensions. We used a standard statistical parametric mapping (one-sample *t* test) to test for significant differences between left and midline trials, and between right and midline trials, over the entire 3D scalp-time volume.

**Dynamic Causal Modeling.** Dynamic Causal Modeling of evoked responses is a model-based method for estimating the coupling between the areas of a cortical network and how this coupling changes with experimental context (David et al., 2006; Kiebel et al., 2006). This context-dependent connectivity is referred to as effective connectivity and is defined as the directed influence one neuronal population exerts over another at the synaptic or laminar level (Friston et al., 2003). DCMs use biologically informed neural-mass models (David et al., 2006) that summarize the neuronal dynamics, within an electromagnetic source, as the average activity over the neuronal populations of the cortical column. Each cortical source comprises excitatory pyramidal cells, as well as excitatory spiny stellate cells and inhibitory interneurons (basket cells) according to the Jansen and Rit model (Jansen and Rit, 1995). The connectivity between cortical areas conforms to the laminar origins and targets described by Felleman and Van Essen (1991) and comprise three types of connections: forward, backward, and lateral. Forward connections are excitatory and drive activity in higher levels of the cortical hierarchy in a feedforward fashion. They originate predominantly from the pyramidal cells in superficial layers (L2/3) and target granular layer 4. Backward connections are inhibitory and provide modulatory feedback to lower levels. They originate mainly in deep layers (L5/6) and target both deep and superficial layers. Lateral connections enable interhemispheric integration between homotopic areas, originate in agranular layers, and target all layers (David et al., 2006). Both extrinsic (between-area) and intrinsic (within-area) connections can change with experimental context (Kiebel et al., 2007).

A DCM is specified in terms of its state equation modeling neuronal dynamics and an observation model generating the measured electromagnetic signal  $y$ . The state equation

$$\dot{x} = f(x, u, \theta)$$

describes how the activity  $x$  in each neuronal population of the network evolves as a function of activity in another population and experimental manipulations  $u$ . This equation is parameterized in terms of the coupling strengths  $\theta$  of intrinsic and extrinsic forward, backward, and lateral connections. The observation model uses a spatiotemporal formulation of a conventional equivalent current dipole (ECD) forward model

$$y = L(\varphi) x_0 + \varepsilon$$

which summarizes the expression of superficial pyramidal cell depolarization  $x_0$  on the EEG sensors with additive Gaussian error  $\varepsilon$ . Each source in the network is modeled as a dipole whose locations and orientations  $\varphi$  parameterize the electromagnetic lead-field matrix  $L$  (Kiebel et al., 2006).

The ensuing lead field was based on a boundary element method (BEM) head model to describe the cortical sheet and the propagation of the electric voltage through the tissue and cranial layers onto the scalp surface (Mosher et al., 1999).

**Bayesian inference.** DCMs are estimated using variational Bayes (Friston et al., 2007). Given a model  $m$ , specified in terms of its prior density  $p(\vartheta|m)$ , and data  $y$ , this furnishes both the posterior density  $p(\vartheta|y,m)$  of the connection strengths  $\vartheta$  and the marginal likelihood of the model itself, known as the model evidence

$$p(y|m) = \int p(y|\vartheta,m) p(\vartheta|m) d\vartheta.$$

Using a Laplace approximation to the posterior density  $q(\vartheta) \approx p(\vartheta|y,m)$ , the posterior means  $\hat{\vartheta}$  and covariances  $\hat{\Sigma}$  are estimated iteratively by maximizing a lower bound on the log-evidence  $\ln p(y|m)$ , formulated as a Newton search on the (negative) free energy  $F$  of model  $m$

$$F = \int q(\vartheta) \ln p(y,\vartheta) d\vartheta - \int q(\vartheta) \ln q(\vartheta) d\vartheta.$$

This renders the free energy an approximation to the log-evidence  $F \approx \ln p(y|m)$ . The first term is the expected log joint density of data  $y$  and parameters  $\vartheta$ . The second term is the (differential) entropy of the model. Both quantities are expectations under the approximate posterior density. The free energy can thus be decomposed into an *accuracy* minus a *complexity* term. These jointly summarize the optimality of a set of parameters (model) in explaining the data as a balance between parameter fit and the cost incurred by increasing the model's complexity (Penny, 2012). This prevents overfitting data  $y$  by penalizing a more complex model in the presence of parameter redundancy with strong correlation in the posterior density, leading to a preference for the simpler model or explanation of the data. The Bayesian model evidence can therefore be viewed as a formalization of the principle of Occam's razor (MacKay, 2003). Under prior assumptions about the models that define a hypothesis space, the model evidence furnishes the posterior probability of the model itself  $p(m|y)$ . Once the model evidence has been obtained, DCMs are compared using Bayesian model comparison (Penny et al., 2004). We used a fixed-effects approach to Bayesian model selection to determine which model of auditory space perception best explains observed responses. In other words, we assumed all subjects have the same network architecture, but different connection strengths (Stephan et al., 2009). Model comparison was based on the log Bayes factor: the difference in the log-evidence of two alternative models, or families of models:  $\ln p(y|m_1) - \ln p(y|m_2)$ , where a value of 3 corresponds to strong evidence for one model or a posterior probability  $p(m|y) > 0.95$  (Kass and Raftery, 1995). We used a uniform prior over the model space to reflect the assumption that our competing hypotheses were a priori equally plausible.

**Network model specification.** We specified a set of anatomically motivated network models that describe the effective connectivity between temporal, frontal, and parietal sources. These models mapped onto our set of alternative hypotheses about the corticocortical networks that mediate perception of auditory space. Specifically, each model represented a version of either orientation bias, which posits a contralateral deployment of connectivity, or right-hemispheric dominance, which posits a bilateral deployment of connectivity for objects in the right hemispace. In addition, each model made different assumptions about the type of connections (forward and backward) that embody hemispheric symmetry or asymmetry. The anatomical structure of these networks was motivated by neuroimaging studies that have localized the primary auditory cortex (Rademacher et al., 2001) and the superior temporal gyrus (Opitz et al., 2002) and indicated a crucial role for the inferior frontal and inferior parietal cortex in audiospatial perception (Griffiths et al., 1998; Bushara et al., 1999; Maeder et al., 2001). We incorporated this anatomical knowledge by setting the prior mean location of the dipoles—used to summarize each cortical source—to the following coordinates in MNI space: left Heschl's gyrus [−42 −22 7], right Heschl's gyrus [46 −14 8], left superior

temporal gyrus [−61 −32 8], right superior temporal gyrus [59 −25 8], left inferior frontal gyrus [−46 28 8], right inferior frontal gyrus [46 28 8], left inferior parietal cortex [−49 −38 38], and right inferior parietal cortex [57 −38 42]. The networks that defined our model space thus varied over three factors: (1) cortical hierarchy—Heschl's gyrus (A1), superior temporal gyrus (STG), inferior frontal gyrus (IFG), and inferior parietal cortex (IPC); (2) type of connection—forward, recurrent (forward and backward), and lateral (interhemispheric); (3) hemispheric laterality—left lateralized, right lateralized or bilateral.

All networks received afferent input to primary auditory cortex via the medial geniculate nucleus of the thalamus. The models increased in hierarchical complexity through the addition of cortical areas. The first set of models included either forward or reciprocal connections that coupled A1 to STG in the right hemisphere only, the left hemisphere only, or in both hemispheres. In more complex models, either forward or reciprocal connections coupled STG to IFG in the right hemisphere only, the left hemisphere only, or in both hemispheres. In the last set of models, either forward or reciprocal connections coupled IFG and IPC in the right hemisphere only, the left hemisphere only, or in both hemispheres. In this way, each model mapped onto an explicit version of orientation bias or right-hemispheric dominance. The anatomical basis of this frontoparietal connectivity has recently been established in humans via the third branch of the superior longitudinal fasciculus (Thiebaut de Schotten et al., 2011). This ventral branch connects the frontal and parietal areas that are commonly activated during automatic reorienting of spatial attention in vision (Corbetta and Shulman, 2002). We entertained spatial deviancy effects (left vs midline or right vs midline) on all of these extrinsic connections. Furthermore, the bilateral intrinsic connections at the first hierarchical level allowed the local microcircuitry within auditory cortex to change between experimental conditions (Kiebel et al., 2007). This intrinsic connectivity furnishes an estimate of the effect of stimulus laterality within primary auditory cortex and is expected to have a bilateral effect with a certain degree of lateralization (von Kriegstein et al., 2008). Finally, reciprocal connections between left and right parietal areas explicitly tested the hypothesis of interhemispheric integration via posterior transcallosal projections (Pandya et al., 1971). This hypothesis was motivated by the orientation bias model and is supported by experimental evidence for interhemispheric integration, where the right frontoparietal network exerts modulatory control over left parietal cortex during visuospatial attention (Koch et al., 2011).

We modeled the data during the poststimulus period 0–300 ms. This period encompasses components of the evoked response that are assumed to reflect the detection of a change in the stimulus location (Paavilainen et al., 1989) and a subsequent bottom-up attentional reorienting to the left or the right hemispace (Polich, 2007). Spatial deviancy is modeled by differences in (or modulations of) coupling strength. These condition-specific differences are constant over peristimulus time, rendering the estimates of effective connectivity time-invariant. This means that we do not model changes in coupling for every time bin, but we estimate one coupling parameter for the entire poststimulus time period. However, the condition-specific changes in connectivity can be expressed early or late in peristimulus time. Our previous work demonstrated that changes in the connectivity of “sensory” sources are generally manifest in early, bottom-up responses (observed as P50 and N100), which contrasts with late top-down effects (observed as MMN and P300) that are mediated by changes in connectivity higher in the cortical hierarchy (Garrido et al., 2007). These cortical responses appear later because evoked responses take a few hundred milliseconds to penetrate deep into the cortical hierarchy.

## Results

### Statistical parametric mapping of evoked responses in sensor space

Random-effects group analysis of the scalp maps of evoked responses revealed a negative ERP to both left and right stimuli relative to stimuli perceived in the midline (Fig. 2). This negativity resembled the classical mismatch negativity (MMN) and peaked at 148 ms for the left ( $t_{(11)} = 6.5$ ,  $p = 0.023$ ) and at 128 ms



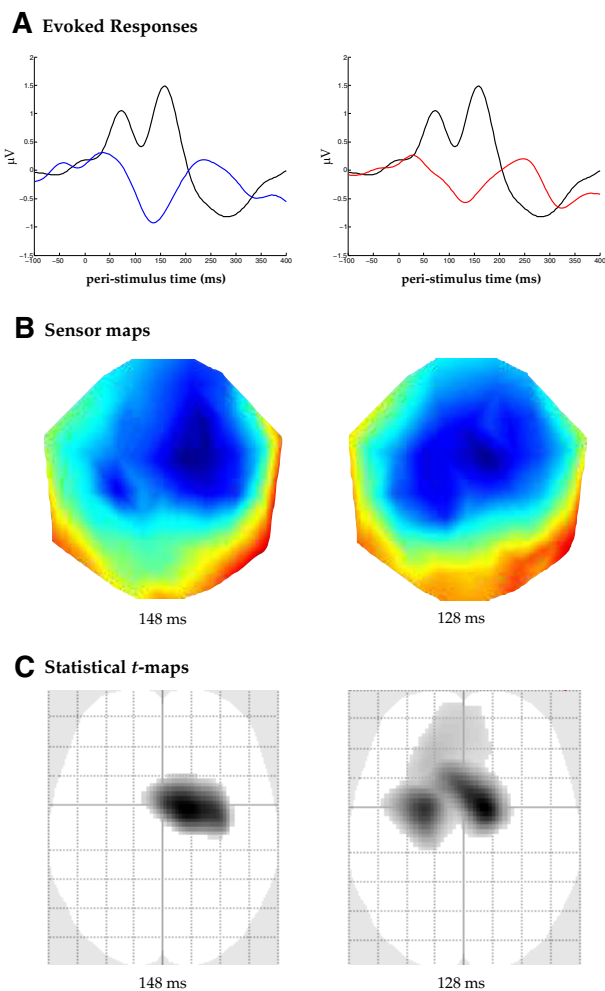


**Figure 2.** *A*, ERPs to left (blue), right (red), and midline (black) stimuli at the EEG sensor with maximal statistical effect. *B*, ERP scalp maps at the time of the maximal peak for left (148 ms) and right (128 ms) spatial deviancy, respectively. *C*, Statistical *t* maps showing the effect of left spatial deviancy (left) and right spatial deviancy (right), thresholded at  $p < 0.001$  uncorrected for visualization.

for the right auditory hemifield ( $t_{(11)} = 9.85$ ,  $p = 0.046$ ), FWE corrected using Random Field Theory (Kilner and Friston, 2010). Responses to both the left and right stimuli had a maximal effect over the right frontocentral scalp. In addition, responses to the right side of space showed a bilateral distribution, whereas responses to the left side of space were significant over the contralateral scalp only. This finding speaks to a hemispheric asymmetry in the cortical processing of right versus left auditory space (Fig. 2C). A later positive ERP was observed for left stimuli peaking at 192 ms over the right parietal scalp ( $t_{(11)} = 5.38$ ,  $p = 0.0001$ ) and for right stimuli peaking at 212 ms with bilateral peaks over the parietal scalp ( $t_{(11)} = 4.26$ ,  $p = 0.001$ ). We interpret this positivity as an early P3a, which is typical in oddball paradigms that induce bottom-up attentional reorienting to salient stimuli (Polich, 2007).

#### Dynamic causal modeling of evoked responses in source space

DCMs were inverted for each subject for two conditions: right spatial deviancy relative to midline and left spatial deviancy relative to midline. The network models that represent our set of prior hypotheses were then compared using Bayesian model selection

(Penny et al., 2004). We first present the results of model comparison of two distinct cortical hierarchies that differ in terms of the anatomical pathways that mediate effective connectivity during audiospatial perception. Using family-level inference (Penny et al., 2010), we compared the frontoparietal family of models to an alternative cortical hierarchy, in which the parietal sources received direct connections from the superior temporal gyrus, without passing through the inferior frontal gyrus. We then present the results of model selection in terms of the network that mediates perception of the left auditory space, the effect of left spatial deviancy, followed by the results of model selection for right auditory space, the effect of right spatial deviancy. This allows for the selection of different cortical networks for the processing of left and right spatial deviancy. Within each network, we summarize the effective connectivity between areas in terms of the percentage change in coupling strength, induced by the spatial deviancy from midline to the left and the right, respectively. Inference on the coupling parameters was performed using classical *t* tests on the posterior means  $\hat{\theta}$  to identify changes in effective connectivity that were significant at the group level in relation to intersubject variability. In this way, we use Bayesian estimation at the single-subject level to furnish posterior estimates of effective connectivity that serve as summary statistics for classical inference at the group level. The significance threshold was set to  $p < 0.05$  with a Bonferroni correction to adjust for multiple comparisons. This adjustment is based on the assumption of independent posterior estimates of the coupling parameters and thus represents the most conservative method to control the family-wise error rate. Finally, after selecting the most likely cortical network engaged by right and left spatial deviancy, we directly compared the orientation bias model and the right-hemisphere dominance model. Here, we modeled both left and right deviant trials and compared models in which coupling changes were symmetric (orientation bias model) or asymmetric (right-hemisphere dominance model) with respect to the laterality of the deviant stimulus. This analysis can be regarded as a formal test of putative hemispheric asymmetries.

#### Cortical hierarchy

We also considered an alternative cortical hierarchy, in which the parietal sources received direct connections from the superior temporal gyrus, without passing through the inferior frontal gyrus. Anatomically, this is a plausible model. However, Bayesian model comparison favored the hierarchical family of models, in which the parietal responses were mediated via the inferior frontal gyrus. This was confirmed with a posterior expected probability  $>0.90$  and an exceedance probability  $>0.99$  in favor of the frontoparietal network (Fig. 3).

#### Left auditory deviancy

The results of Bayesian model selection show that a right-lateralized temporo-fronto-parietal network best explains the brain responses to changes in sound location from the midline to the left side of auditory space. We found strong evidence in favor of this right-lateralized network compared with the set of alternative hypotheses (models), with a posterior model probability  $>0.99$  (Fig. 4). There was a significant increase in the intrinsic (within-area) coupling in right A1 (16.3%;  $t = 4.04$ ,  $p = 0.001$ ), consistent with the stronger contralateral activation shown by von Kriegstein et al. (2008). Recurrent forward and backward connections changed in both hemispheres within temporal cortex. Here, an increase in coupling strength from right A1 to right

STG (50.6%;  $t = 2.76$ ,  $p = 0.009$ ) provides further evidence of a hemispheric lateralization within temporal cortex. Mediated by the reciprocal connections between temporal cortex and the IFG in both hemispheres, right lateralization was confirmed with a large increase in the forward connection (76.7%;  $t = 4.26$ ,  $p = 0.0007$ ) from right IFG to the IPC. Significant increases in coupling were only present in the right hemisphere, contralateral to the stimulus location. Finally, there was evidence for interhemispheric integration through inferior parietal cortices, as revealed by a large increase in the lateral connection from right to left IPC (59.7%;  $t = 4.00$ ,  $p = 0.001$ ). This finding further supports the existing evidence that a right frontoparietal network exerts modulatory control over the left parietal cortex, as observed in visu-

ospatial attention (Koch et al., 2011). The contralateral change in forward connectivity that drives the cortical responses can be expressed early or late in poststimulus time. To illustrate the temporal expression of connectivity changes, we evaluated the influence that each forward connection has on its target source in the right hemisphere, contralateral to the stimulus location (Fig. 4C). This sensitivity analysis evaluated the change in pyramidal cell activity in each of the temporal, frontal, and parietal sources with respect to a change in its afferent forward connection  $\partial x(t)/\partial \theta$ . This effectively discloses the temporal expression of the source activity as a function of the particular connection that drives its responses. The change in the coupling parameter between two regions was set to  $\partial \theta = \exp(-6)$  to provide an appropriate scaling. Note that the responses are normalized for visualization to accommodate differences in scaling among sources. The response in auditory cortex reflects the effect of the thalamic input and is shown for completeness. The activity of superficial pyramidal cells is known to produce the observed EEG/MEG signal and therefore has a direct interpretation in relation to the observed responses. Our results show that the forward connections exert their effects successively later in poststimulus time at progressively higher levels of the cortical hierarchy. Changes in the connectivity between sensory sources within temporal cortex drive early, bottom-up responses that have a temporal correspondence with the classical N100. Conversely, changes in connectivity higher in the cortical hierarchy induce

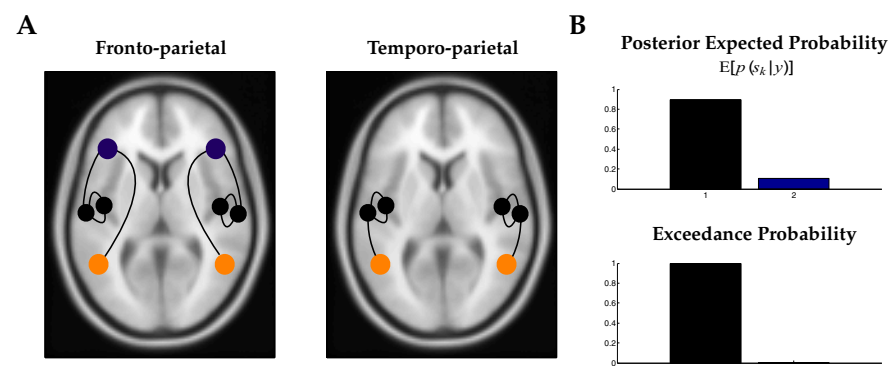


**Figure 3.** *A*, Anatomical structure of the frontoparietal and temporoparietal hierarchies, summarized in terms of the fullest model in each family. The frontoparietal model includes the temporal (black), frontal (blue), and parietal sources (orange) in hierarchical order. The temporoparietal model includes the temporal (black) and parietal sources (orange). *B*, Family-level inference shows strong evidence in favor of a frontoparietal network with a posterior expected probability  $> 0.90$  and exceedance probability  $> 0.99$ .

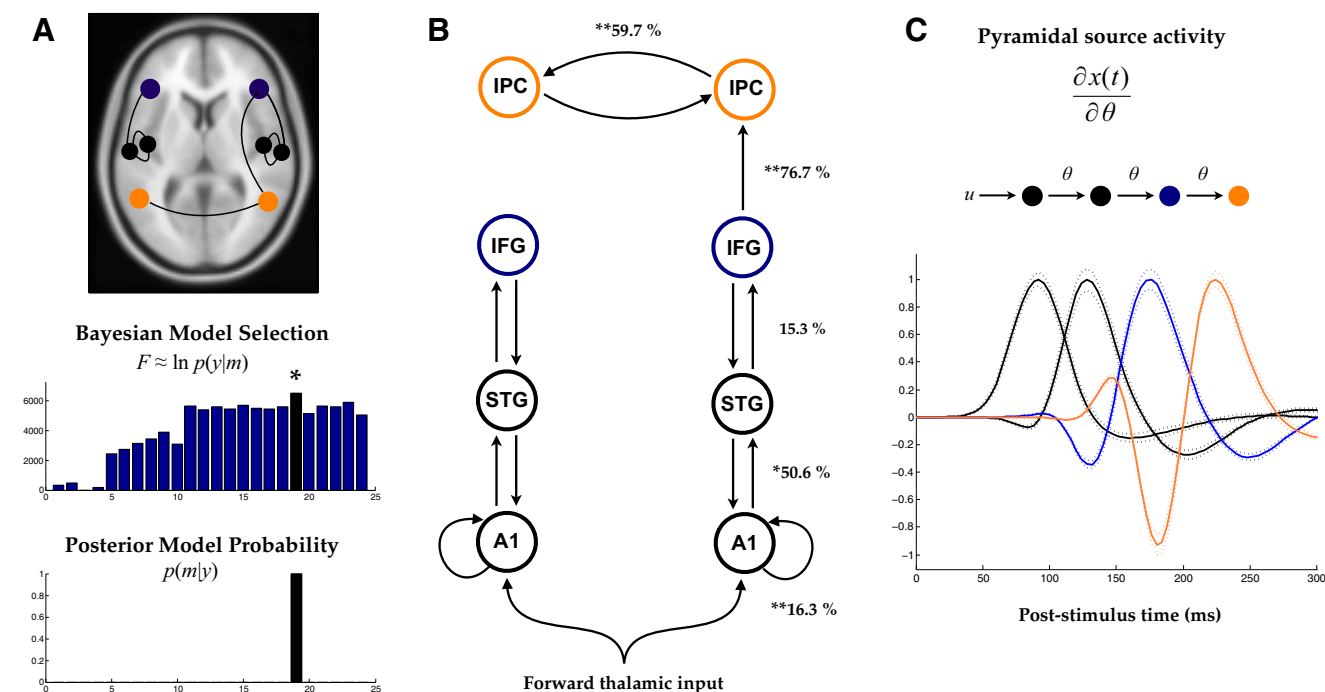


**Figure 4.** *A*, Anatomical architecture of the DCM that best explains the brain responses to changes from midline to the left side of auditory space. This right-lateralized network has the highest log-evidence and a posterior model probability  $> 0.99$ . *B*, Network graph showing percentage changes in effective connectivity that increases selectively in the hemisphere contralateral to sensory stimulation (\* $p < 0.05$ , \*\* $p < 0.05$  Bonferroni corrected). *C*, Average response of temporal, frontal, and parietal sources in the right hemisphere with respect to a change in its forward connection  $\partial x(t)/\partial \theta$ .

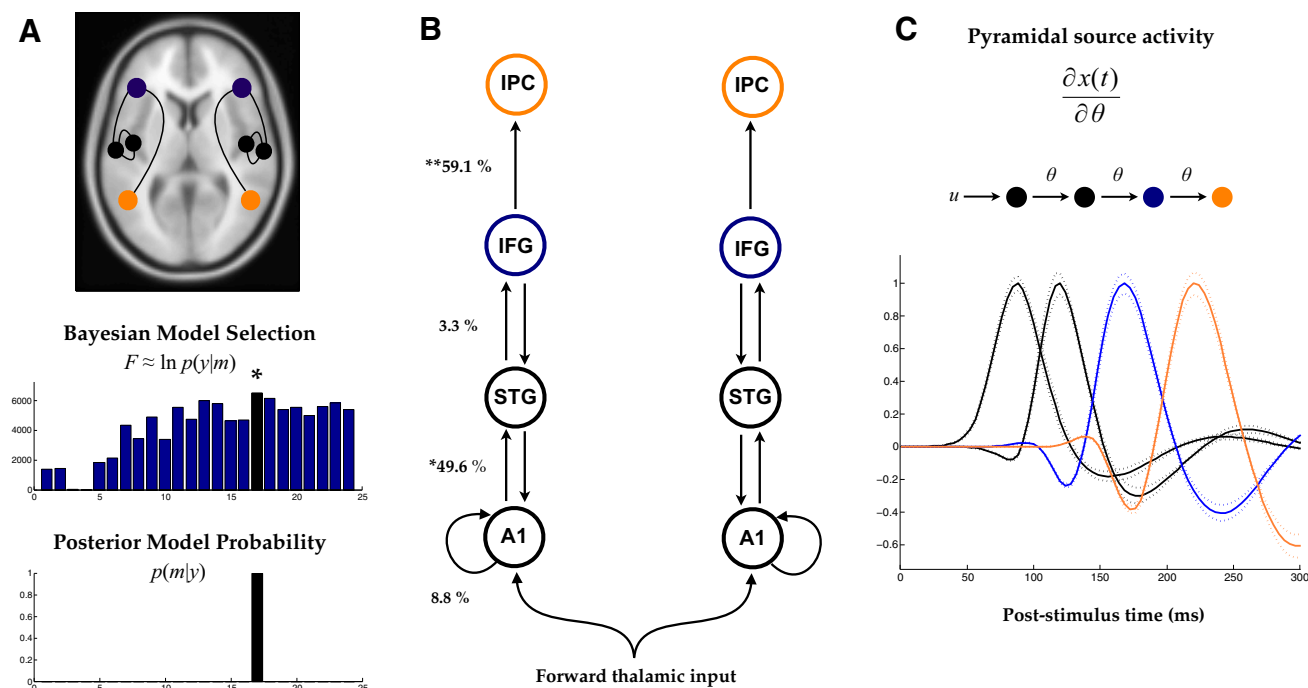


**Figure 5.** *A*, Anatomical architecture of the DCM that best explains the brain responses to changes from midline to the right side of auditory space. This bilateral network has the highest log-evidence and a posterior model probability  $> 0.99$ . *B*, Network graph showing percentage changes in effective connectivity that increases selectively in the hemisphere contralateral to sensory stimulation (\* $p < 0.05$ , \*\* $p < 0.05$  Bonferroni corrected). *C*, Average response of the temporal, frontal, and parietal sources in the left hemisphere with respect to a change in its forward connection  $\partial x(t)/\partial \theta$ .

late effects whose temporal expression matches those of the MMN and P3a.

### Right auditory deviancy

Bayesian model selection showed that a bilateral temporo-fronto-parietal network best explains the brain responses to changes in sound location from the midline to the right side of auditory space. We found very strong evidence in favor of this bilateral network compared with the set of alternative hypotheses, with a posterior model probability  $> 0.99$  (Fig. 5). In terms of its architecture, the network evidenced the same reciprocal connections within temporal cortex and between superior temporal and the inferior frontal cortex reported above. We found a significant increase in the forward connection from left A1 to left STG (49.6%;  $t = 2.29$ ,  $p = 0.02$ ), which mirrors the lateralization observed for perception of the left auditory space. Again, this shows a selective increase in the contralateral forward connection within temporal cortex. Consistent with the right-hemisphere dominance model, we found evidence for a bilateral network that increases the strength of forward connectivity from frontal to parietal cortices. Importantly, within this bilateral network, a selective increase in coupling strength (59.1%;  $t = 3.72$ ,  $p = 0.001$ ) in the left hemisphere suggests a degree of lateralization. This mirrors the increase in coupling between frontal and parietal cortex observed for perception of the opposite side of auditory space. Finally, there was no evidence for interhemispheric integration between parietal cortices, in contrast to our findings for left spatial deviancy. This is consistent with the hypothesis that only the right frontoparietal network modulates the left parietal cortex during the allocation of spatial attention, in contradistinction to mutual modulation between the two hemispheres (Koch et al., 2011). In short, these findings support the right-hemisphere dominance model of audiospatial perception. To

illustrate the temporal expression of connectivity changes contralateral to the stimulus location, we evaluated the influence that each forward connection has on its target area in the left hemisphere using the sensitivity analysis described above (Fig. 5C). The response in auditory cortex reflects the effect of the thalamic input and is shown for completeness. This shows that for both left and right spatial deviancy, the forward connections in the hemisphere contralateral to the side of stimulation exert their effects early and late in poststimulus time at lower and higher levels of the cortical hierarchy, respectively. Note that the early responses in auditory cortex correspond to the classical N100. This reflects the subcortical input from the thalamus that drives the network in a feedforward fashion. The response in the inferior frontal cortex has a temporal expression that matches that of the MMN, which is assumed to reflect the detection of a change in the stimulus location (Paavilainen et al., 1989). Finally, the temporal expression of the parietal response corresponds to the P3a, which is assumed to reflect the attentional reorienting to the *left* or the *right* side of auditory space (Friedman et al., 2001). This is in line with previous evidence that the observed P300 arises from the interaction between frontal and parietal regions (Polich, 2007).

### Orientation bias versus right-hemisphere dominance

Having established the corticocortical network that mediates responses to deviancy in each auditory hemisphere separately, we compared a DCM that embodies an orientation bias model with a DCM that conforms to the right-hemisphere dominance model. This comparison included the trials from both left and right experimental conditions, where we constrained the changes in coupling to be either contralateral to the side of stimulus deviancy, with mutual modulation of the ipsilateral hemisphere (orientation bias model) or to have an asymmetric expression (right-hemisphere dominance model). In the latter model, left

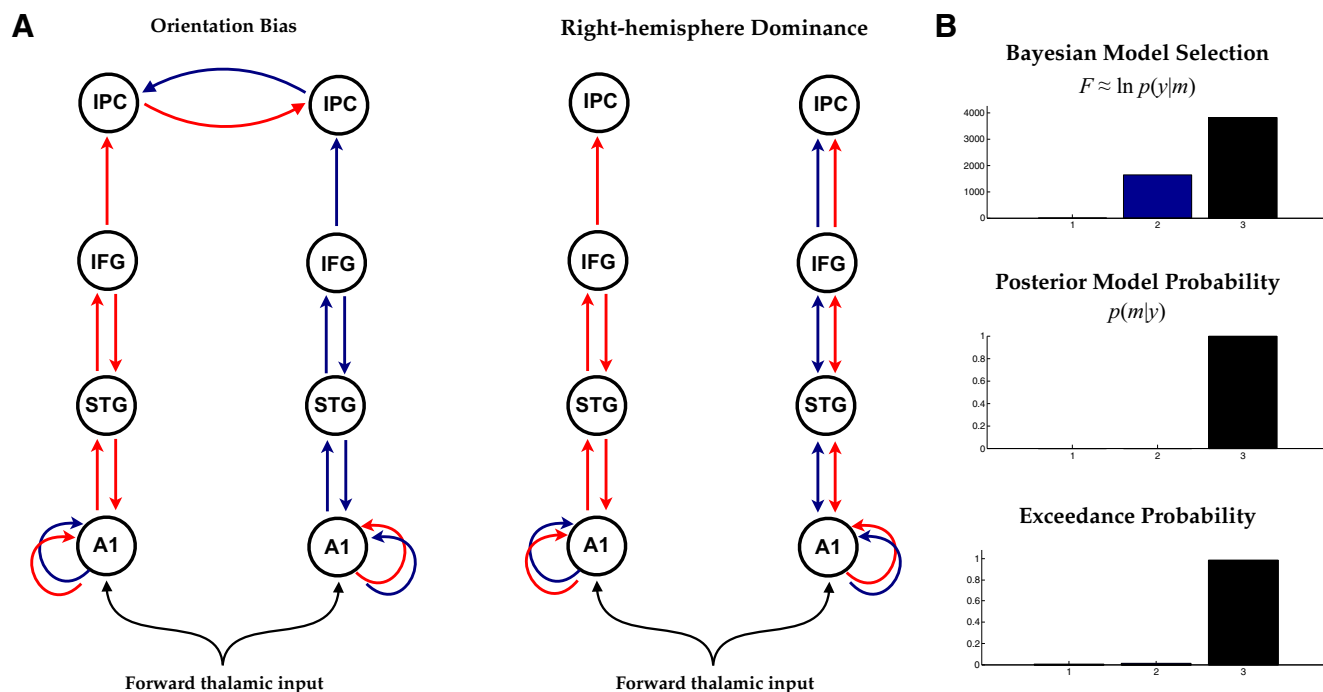


**Figure 6.** **A**, Network graph of the orientation bias model and the right-hemisphere dominance model: right (red) and left (blue) side of stimulus space. **B**, Bayesian model selection showing the (relative) log-evidences of (1) a null model with no change in coupling, (2) the orientation bias model with a contralateral change in coupling, and (3) the right-hemisphere dominance model. A posterior model probability  $> 0.99$  and exceedance probability of  $> 0.98$  is strong evidence in favor of a hemispheric asymmetry.

auditory stimuli modulated connections in the right hemisphere and right auditory stimuli modulated both left and right hemispheres. We tested these alternative hypotheses against a null model that precluded any changes in connectivity. Bayesian model selection provided very strong evidence in favor of an asymmetric coding of space, which conforms to the right-hemisphere dominance model, with a posterior probability  $> 0.99$  and an exceedance probability  $> 0.98$  (Fig. 6).

## Discussion

We formulated competing hypotheses about the cortical networks that mediate audiospatial perception and tested these alternative models using human EEG data. We induced bottom-up attentional reorienting with an auditory location oddball paradigm. Electrophysiological responses to unpredictable, spatially deviant events showed a classical mismatch negativity reflecting change detection (Paavilainen et al., 1989) and a subsequent P3a reflecting attentional reorienting (Polich, 2007). Bayesian model comparison of a set of increasingly complex networks revealed that responses to the left side of space involved the interaction between frontal and parietal regions in the contralateral hemisphere. However, responses to the right side of space were generated by interactions among frontal and parietal cortices in both hemispheres. These results support the idea of a hemispheric asymmetry in a frontoparietal network that is in accordance with the right-hemisphere dominance model originally proposed by Heilman and Van Den Abell (1979) and Mesulam (1981). Interestingly, we found an increase in the interhemispheric connection from right to left parietal cortex. This is in line with existing evidence for a right parietal inhibitory control over the left parietal cortex in visuospatial attention (Koch et al., 2011). In the formal test of hemispheric asymmetries, we directly compared frontoparietal networks that embodied our two alternative hypotheses. Within this asymmetric network, we show that a selec-

tive increase in effective connectivity establishes a crucial role for the contralateral connections in encoding the location of a stimulus in auditory space. In this sense, there is evidence for lateralization within the right-hemisphere dominant network.

## Attention, saliency, and precision

In terms of the implications of our results for computational theories of perception and attention, our findings are consistent with the attentional redeployment that would be expected under hierarchical predictive coding. Under this formulation of the brain, perception corresponds to inferring the (hidden) causes of sensory inputs by minimizing a free-energy bound on the surprise  $-\ln p(\tilde{s}|m)$  about sensations  $\tilde{s}$  given a generative model  $m$  of the world (Friston and Kiebel, 2009). This corresponds to maximizing the evidence  $\ln p(\tilde{s}|m)$  of a model of the world. Neurophysiologically, the explicitly hierarchical structure of these models is likely implemented in the form of message-passing between higher and lower levels of the cortical hierarchy as described above. Here, backward connections provide lower levels with predictions in the form of prior beliefs about perceptual states, whereas forward connections carry prediction errors to inform higher levels as to the most likely stimulus perception (Bastos et al., 2012). Importantly, both higher-level predictions and lower-level prediction error are weighted by their relative precision. Our main finding was a profound increase in the strength of forward connectivity. In other words, the relative sensitivity or gain of excitatory spiny stellate populations to feedforward afferents increased markedly when unpredicted stimuli appeared in the contralateral hemifield. This finding is entirely consistent with recent proposals that visual attention is mediated by the precision of prediction errors encoded by the postsynaptic gain of pyramidal cells in superficial layers, which receive inputs from spiny stellate cells (Feldman and Friston, 2010). The idea is that unanticipated sensory stimuli are surprising and thus induce



a redeployment of attentional gain through top-down neuromodulatory mechanisms. This attentional gain is controlled by the precision (inverse variance) of prediction errors, which enhances the salience of ascending prediction errors that inform higher levels during perceptual inference. Effectively, this increases the effect of sensory prediction errors on hierarchical representations of the sensorium, relative to descending prior predictions. Mathematically, the weighting of data in relation to their precision is central to Bayesian inference and provides a principled way of understanding exogenous attention from a computational perspective: as the optimization of the weight given to forward prediction errors, relative to backward predictions, during perceptual uncertainty. The selective increases in connectivity reported above for left and right spatial deviancy, respectively, can be seen as modeling context-dependent increases in postsynaptic gain, which are expressed in terms of an increase in the strength of forward connections that convey precision-weighted prediction errors. This context-dependent expression of the forward connectivity points to attentional gain modulation as an integral part of the cortical hierarchies that mediate perception. This interpretation fits with recent dynamic causal modeling studies of oddball responses that have been interpreted in terms of changes in connectivity at specific levels of the auditory hierarchy (Garrido et al., 2009). From the point of view of our experiment, the probabilistic nature of stimuli and the specialized neuronal systems that mediate perception are inseparable, in the sense that an unpredictable stimulus is expected to increase connectivity within the particular network that is specialized for processing the stimulus in question. Note that while both left and right deviants are infrequent, only the left (not the right) deviant elicits a right-lateralized response. This cannot be explained on the basis of rarity, as both left and right deviants are equally infrequent. In short, we do not believe that probabilistic stimuli evoke lateralized responses per se, but rather do so within the network that is specialized for predicting and minimizing prediction error (free energy) with respect to a particular sensory context.

### Bayesian model inference

Previous noninvasive studies of audiospatial perception in humans have either used EEG to describe ERPs at the sensor level (Paavilainen et al., 1989; Deouell et al., 2006) or dipole models that focused on accurate localization of temporally specific responses in auditory cortex (Kaiser et al., 2000; Krumbholz et al., 2007). Other studies have investigated audiospatial perception with spatially resolved BOLD fMRI (Griffiths et al., 1998; Maeder et al., 2001; Zatorre et al., 2002; Krumbholz, 2005), which effectively low-pass filters fast neuronal processes. The anatomical correspondence between the observed scalp EEG topography and the neuronal sources that generated these observations does not have a unique solution, especially in the case of multiple simultaneous sources. In other words, it is not possible to infer where in the brain signals were generated without prior constraints on the solution (Baillet et al., 2001). We used a Bayesian framework to estimate the log-evidence of a set of alternative network models (hypotheses), summarized in terms of a set of ECDs in source space. This is not possible with traditional ERP analyses because they operate at the level of the EEG channels. With a Bayesian approach to the identification of effective connectivity, we were able to explicitly test alternative network architectures above and beyond voxelwise analyses where statistical inference only pertains to any one region in the brain. More specifically, the formal identification of a network in the brain, given electrophysiological

or neuroimaging data, is possible because of the multivariate nature of the log-evidence used for model selection. This is because the free-energy approximation to the log-evidence summarizes the optimality of a model in explaining the data as a balance between accuracy and complexity (Penny, 2012). We directly address the question of hemispheric asymmetries by comparing a set of well defined alternative hypotheses (models) using their log-evidence. When formulating these alternative hypotheses, we used the results from previous neuroimaging studies to inform our spatiotemporal dipole models in terms of the prior locations of cortical sources (Kiebel et al., 2006). In this way, we have formally incorporated the existing anatomical knowledge in the form of prior beliefs about the cortical network that mediates audiospatial perception and tested our alternative hypotheses given the data in a Bayes-optimal fashion.

### Neglect as a disconnection syndrome

Unilateral spatial neglect typically results from a lesion in the right hemisphere that leaves the patient unable to attend to the left side of the sensorium (Mesulam, 1999). Our results suggest that the more frequent and severe left-sided neglect is a consequence of right-hemisphere dominance of spatial attention as a general systems property of the brain. The frontoparietal network identified above is characterized by an asymmetric coding of auditory space, embodied in the effective connectivity that changes as a function of stimulus laterality. Crucially, this asymmetry is predicted by recent anatomical evidence in humans showing that the superior longitudinal fasciculus, which connects frontal and parietal cortices, has a right-hemisphere dominance: the volume of white matter tracts in the right hemisphere correlated positively with performance during detection of targets in the left compared with the right visual hemifield (Thiebaut de Schotten et al., 2011). There is a great heterogeneity in the lesion profiles of neglect patients (Molenberghs et al., 2012) and the fact that lesions in temporal, frontal, or parietal cortex all lead to a similar attentional deficit (Verdon et al., 2010) points to the idea of unilateral neglect as a “disconnection syndrome” (Bartolomeo et al., 2007). This would explain why unilateral neglect, characterized neuropsychologically as a general impairment in the allocation of attention to one particular side of the sensorium, can result from lesions at different anatomical nodes. Or, indeed, as a result of the disruption of fiber pathways of the frontoparietal network that mediates top-down and bottom-up attention (Corbetta and Shulman, 2011) via the superior longitudinal fasciculus (Thiebaut de Schotten et al., 2011). Future studies in neglect patients will test this idea with the sort of connectivity models used here.

### References

- Baillet S, Mosher JC, Leahy RM (2001) Electromagnetic brain mapping. *IEEE Signal Proc Mag* 18:14–30. [CrossRef](#)
- Bartolomeo P, Thiebaut de Schotten M, Doricchi F (2007) Left unilateral neglect as a disconnection syndrome. *Cereb Cortex* 17:2479–2490. [CrossRef Medline](#)
- Bastos AM, Usrey WM, Adams RA, Mangun GR, Fries P, Friston KJ (2012) Canonical microcircuits for predictive coding. *Neuron* 76:695–711. [CrossRef Medline](#)
- Brunetti M, Della Penna S, Ferretti A, Del Gratta C, Cianflone F, Belardinelli P, Caulo M, Pizzella V, Olivetti Belardinelli M, Romani GL (2008) A frontoparietal network for spatial attention reorienting in the auditory domain: a human fMRI/MEG study of functional and temporal dynamics. *Cereb Cortex* 18:1139–1147. [CrossRef Medline](#)
- Bushara KO, Weeks RA, Ishii K, Catalan MJ, Tian B, Rauschecker JP, Hallett M (1999) Modality-specific frontal and parietal areas for auditory and visual spatial localization in humans. *Nat Neurosci* 2:759–766. [CrossRef Medline](#)



- Corbetta M, Shulman GL (2002) Control of goal-directed and stimulus-driven attention in the brain. *Nat Rev Neurosci* 3:201–215. [Medline](#)
- Corbetta M, Shulman GL (2011) Spatial neglect and attention networks. *Annu Rev Neurosci* 34:569–599. [CrossRef Medline](#)
- David O, Kiebel SJ, Harrison LM, Mattout J, Kilner JM, Friston KJ (2006) Dynamic causal modeling of evoked responses in EEG and MEG. *Neuroimage* 30:1255–1272. [CrossRef Medline](#)
- Deouell LY, Parnes A, Pickard N, Knight RT (2006) Spatial location is accurately tracked by human auditory sensory memory: evidence from the mismatch negativity. *Eur J Neurosci* 24:1488–1494. [CrossRef Medline](#)
- Driver J, Mattingley JB (1998) Parietal neglect and visual awareness. *Nat Neurosci* 1:17–22. [CrossRef Medline](#)
- Feldman H, Friston KJ (2010) Attention, uncertainty, and free-energy. *Front Hum Neurosci* 4:215. [CrossRef Medline](#)
- Felleman DJ, Van Essen DC (1991) Distributed hierarchical processing in the primate cerebral cortex. *Cereb Cortex* 1:1–47. [CrossRef Medline](#)
- Friedman D, Cycowicz YM, Gaeta H (2001) The novelty P3: an event-related brain potential (ERP) sign of the brain's evaluation of novelty. *Neurosci Biobehav Rev* 25:355–373. [CrossRef Medline](#)
- Friston K, Kiebel S (2009) Predictive coding under the free-energy principle. *Philos Trans R Soc Lond B Biol Sci* 364:1211–1221. [CrossRef Medline](#)
- Friston KJ, Harrison L, Penny W (2003) Dynamic causal modelling. *Neuroimage* 19:1273–1302. [CrossRef Medline](#)
- Friston K, Mattout J, Trujillo-Barreto N, Ashburner J, Penny W (2007) Variational free energy and the Laplace approximation. *Neuroimage* 34:220–234. [CrossRef Medline](#)
- Fritz JB, Elhilali M, David SV, Shamma SA (2007) Auditory attention—focusing the searchlight on sound. *Curr Opin Neurobiol* 17:437–455. [CrossRef Medline](#)
- Garrido MI, Kilner JM, Kiebel SJ, Friston KJ (2007) Evoked brain responses are generated by feedback loops. *Proc Natl Acad Sci U S A* 104:20961–20966. [CrossRef Medline](#)
- Garrido MI, Kilner JM, Kiebel SJ, Friston KJ (2009) Dynamic causal modeling of the response to frequency deviants. *J Neurophysiol* 101:2620–2631. [CrossRef Medline](#)
- Griffiths TD, Rees G, Rees A, Green GG, Witton C, Rowe D, Büchel C, Turner R, Frackowiak RS (1998) Right parietal cortex is involved in the perception of sound movement in humans. *Nat Neurosci* 1:74–79. [CrossRef Medline](#)
- Heffner RS, Masterton RB (1990) Sound localization in mammals: brainstem mechanisms. In: *Comparative perception*, Vol 1 (Berkley MA, Stebbins WC, eds), pp 285–314. New York: Wiley.
- Heilman KM, Van Den Abell T (1979) Right hemispheric dominance for mediating cerebral activation. *Neuropsychologia* 17:315–321. [CrossRef Medline](#)
- Irvine DRF (1986) *The auditory brainstem*. Springer: Berlin.
- Jansen BH, Rit VG (1995) Electroencephalogram and visual-evoked potential generation in a mathematical model of coupled cortical columns. *Biol Cybern* 73:357–366. [CrossRef Medline](#)
- Kaiser J, Lutzenberger W, Preissl H, Ackermann H, Birbaumer N (2000) Right-hemisphere dominance for the processing of sound-source lateralization. *J Neurosci* 20:6631–6639. [Medline](#)
- Kass RE, Raftery AE (1995) Bayes factors. *J Am Stat Assoc* 90:773–795. [CrossRef](#)
- Kiebel SJ, David O, Friston KJ (2006) Dynamic causal modelling of evoked responses in EEG/MEG with lead field parameterization. *Neuroimage* 30:1273–1284. [CrossRef Medline](#)
- Kiebel SJ, Garrido MI, Friston KJ (2007) Dynamic causal modelling of evoked responses: the role of intrinsic connections. *Neuroimage* 36:332–345. [CrossRef Medline](#)
- Kilner JM, Friston KJ (2010) Topological inference for EEG and MEG. *Ann Appl Stat* 4:1272–1290. [CrossRef](#)
- Kinsbourne M (1970) The cerebral basis of lateral asymmetries in attention. *Acta Psychologica* 33:193–201. [CrossRef Medline](#)
- Kinsbourne M (1977) Hemi-neglect and hemisphere rivalry. *Adv Neurol* 18:41–49. [Medline](#)
- Koch GG, Cercignani M, Bonni S, Giacobbe V, Bucci G, Versace V, Calta-girone C, Bozzali M (2011) Asymmetry of parietal interhemispheric connections in humans. *J Neurosci* 31:8967–8975. [CrossRef Medline](#)
- Krumbholz K, Schönwiesner M, von Cramon DY, Rüsamen R, Shah NJ, Zilles K, Fink GR (2005) Representation of interaural temporal information from left and right auditory space in the human planum temporale and inferior parietal lobe. *Cereb Cortex* 15:317–324. [CrossRef Medline](#)
- Krumbholz K, Hewson-Stoate N, Schönwiesner M (2007) Cortical response to auditory motion suggests an asymmetry in the reliance on inter-hemispheric connections between the left and right auditory cortices. *J Neurophysiol* 97:1649–1655. [Medline](#)
- MacKay DJC (2003) *Information theory, inference and learning algorithms*. Cambridge, UK: Cambridge UP.
- Maeder PP, Meuli RA, Adriani M, Bellmann A, Fornari E, Thiran JP, Pittet A, Clarke S (2001) Distinct pathways involved in sound recognition and localization: a human fMRI study. *Neuroimage* 14:802–816. [CrossRef Medline](#)
- Mesulam MM (1981) A cortical network for directed attention and unilateral neglect. *Ann Neurol* 10:309–325. [CrossRef Medline](#)
- Mesulam MM (1999) Spatial attention and neglect: parietal, frontal and cingulate contributions to the mental representation and attentional targeting of salient extrapersonal events. *Philos Trans R Soc Lond B Biol Sci* 354:1325–1346. [CrossRef Medline](#)
- Molenberghs P, Sale MV, Mattingley JB (2012) Is there a critical lesion site for unilateral spatial neglect? A meta-analysis using activation likelihood estimation. *Front Hum Neurosci* 6:78. [CrossRef Medline](#)
- Mosher JC, Leahy RM, Lewis PS (1999) EEG and MEG: forward solutions for inverse methods. *IEEE Trans Biomed Eng* 46:245–259. [CrossRef Medline](#)
- Opitz B, Rinne T, Mecklinger A, von Cramon DY, Schröger E (2002) Differential contribution of frontal and temporal cortices to auditory change detection: fMRI and ERP results. *Neuroimage* 15:167–174. [CrossRef Medline](#)
- Paavilainen P, Karlsson ML, Reinikainen K, Näätänen R (1989) Mismatch negativity to change in spatial location of an auditory stimulus. *Electroencephalogr Clin Neurophysiol* 73:129–141. [CrossRef Medline](#)
- Pandya DN, Karol EA, Heilbronn D (1971) The topographical distribution of interhemispheric projections in the corpus callosum of the rhesus monkey. *Brain Res* 32:31–43. [CrossRef Medline](#)
- Penny WD (2012) Comparing dynamic causal models using AIC, BIC and free energy. *Neuroimage* 59:319–330. [CrossRef Medline](#)
- Penny WD, Stephan KE, Mechelli A, Friston KJ (2004) Comparing dynamic causal models. *Neuroimage* 22:1157–1172. [CrossRef Medline](#)
- Penny WD, Stephan KE, Daunizeau J, Rosa MJ, Friston KJ, Schofield TM, Leff AP (2010) Comparing families of dynamic causal models. *PLoS Comput Biol* 6:e1000709. [CrossRef Medline](#)
- Polich J (2007) Updating P300: an integrative theory of P3a and P3b. *Clin Neurophysiol* 118:2128–2148. [CrossRef Medline](#)
- Rademacher J, Morosan P, Schormann T, Schleicher A, Werner C, Freund HJ, Zilles K (2001) Probabilistic mapping and volume measurement of human primary auditory cortex. *Neuroimage* 13:669–683. [CrossRef Medline](#)
- Stephan KE, Penny WD, Daunizeau J, Moran RJ, Friston KJ (2009) Bayesian model selection for group studies. *Neuroimage* 46:1004–1017. [CrossRef Medline](#)
- Thiebaut de Schotten T, Dell'Acqua F, Forkel SJ, Simmons A, Vergani F, Murphy DG, Catani M (2011) A lateralized brain network for visuospatial attention. *Nat Neurosci* 14:1245–1246. [CrossRef Medline](#)
- Thompson SK, von Kriegstein K, Deane-Pratt A, Marquardt T, Deichmann R, Griffiths TD, McAlpine D (2006) Representation of interaural time delay in the human auditory midbrain. *Nat Neurosci* 9:1096–1098. [CrossRef Medline](#)
- Verdon V, Schwartz S, Lovblad KO, Hauert CA, Vuilleumier P (2010) Neuroanatomy of hemispatial neglect and its functional components: a study using voxel-based lesion-symptom mapping. *Brain* 133:880–894. [CrossRef Medline](#)
- von Kriegstein K, Griffiths TD, Thompson SK, McAlpine D (2008) Responses to interaural time delay in human cortex. *J Neurophysiol* 100:2712–2718. [CrossRef Medline](#)
- Wager TD, Keller MC, Lacey SC, Jonides J (2005) Increased sensitivity in neuroimaging analyses using robust regression. *Neuroimage* 26:99–113. [CrossRef Medline](#)
- Zatorre RJ, Bouffard M, Ahad P, Belin P (2002) Where is “where” in the human auditory cortex? *Nat Neurosci* 5:905–909. [CrossRef Medline](#)